



Review Article

Received: July 19, 2021

Accepted: October 13, 2021

Published: October 13, 2021

ISSN 2658-5553

## Pipe erosion under multiphase flow. A review

Taheri Fard, Ali Reza \*<sup>1</sup> 

<sup>1</sup> Peter the Great St. Petersburg Polytechnic University, Saint-Petersburg, Russian Federation  
Correspondence:\* email [alireza\\_taherifard@yahoo.com](mailto:alireza_taherifard@yahoo.com); contact phone [+79819312783](tel:+79819312783)

### Keywords:

Erosion; Sand particle; Turbulent flow; Boundary layer flow; Multiphase flow; Fluid mechanic; Erosion modeling; CFD modeling; Mass transfer

### Abstract:

Sand is often produced simultaneously with oil, and gas, which causes a significant issue in the petroleum industry. Therefore, sand production in gas and oil extraction needs to be studied thoroughly as it can cause many problems. Three problems arise among all: reducing pressure, pipe obstruction, and erosion. The second is a complicated, impersonal process in which material is eliminated from the pipe by the replicated effect of sand particles. Consequently, the pipe undergoes an erosion process. Erosion in pipes can lead to failures in pipelines, economic damage, and environmental problems. Hence, it is crucial to identify the parameters which determine erosion events as well as modeling them. This article provides an overview of the essential factors causing erosion and an explanation of the current erosion equations. It also describes experimental, and mechanical models of pipe erosion prediction. Moreover, it explains the modeling of fluid erosion dynamics as a comprehensive fragmentation study method. Ultimately, potential limits and shortcomings regarding erosion are demonstrated.

## 1 Introduction

It is ubiquitous to extract sand from gas, and oil pipelines. Sand production can occur severe economic, and environmental damage. Sand production can cause erosion, dumping, occlusion in pipelines, sand scale erosion, erosion, and other problems. The way to deal with sand is to eradicate it with the help of sand screens, and gravel filters. Nonetheless, complex technical, and financial issues are involved in the elimination or control of sand production, especially in flood conditions. For instance, the sand screen cannot block the entry of small grains (less than 50  $\mu\text{m}$ ) from being driven along with gas or oil. These tiny particles can get through sand filters or obstruct the screen in other zones leads erosion at a high rate. This process can broaden the holes in the sieve, which allows larger particles to pass through, wear away the screen, and eventually fail. One of the vital outcomes of sand extraction is erosion. Sand erosion may give rise to equipment failure, pipe leakage, which leads to environmental damage.

Hence, estimating the particle erosion rate is a valuable instrument to design, and pick up the facilities to avoid failure. However, the solid decomposition of gases and liquids is challenging to predict. Despite all sources used for researching erosion, the mechanisms of solid particles still are not thoroughly comprehended. Therefore, the researchers have presented different strategies. Overall, estimating erosion models can be categorized into three: experimental, and mechanical, and CFD. Since predicting erosion is complicated, most of the researchers are studying erosion using the combination of all. The primary purpose of this article is to provide all the details. The paper is categorized as in the following. Section 2 considers essential parameters for the warning of particle erosion and its effect. Section 3 is separated into various subsections, which commence with the review of accessible equations in the publications. Then, different practices, and mechanistic erosion prognostication models are discussed. In the end, CFD-based modeling of erosion is considered. In Section 4, an assessment of some of the investigated models is demonstrated.

Taheri Fard, A.

Pipe erosion under multiphase flow. A review;

2021; *AlfaBuild*; Volume 19 Article No 1901. doi: 10.57728/ALF.19.1

## 2 Mechanism of solid particle erosion

When the sand particles hit the metal's surface, some of the metal is removed. When the particles reach the surface, scars appear, and many researchers have studied these spots to elaborate the mechanism of erosion damage [1]. The erosion rate is mainly determined by the metal flexibility and the speed of the solid particles. Breakable materials are destroyed by the cracking mechanisms, while plant materials are crushed by scratch or deformation mechanisms (Fig.1) [2]–[4]. Pursuant to Finnie, the amount of surface material destroyed by solids in the liquid stream depends on the fluid flow conditions and the material removal mechanism. For pliant materials, it is possible to provide a means by which the removal of the material depends on the speed, and direction of the falling particles [5].

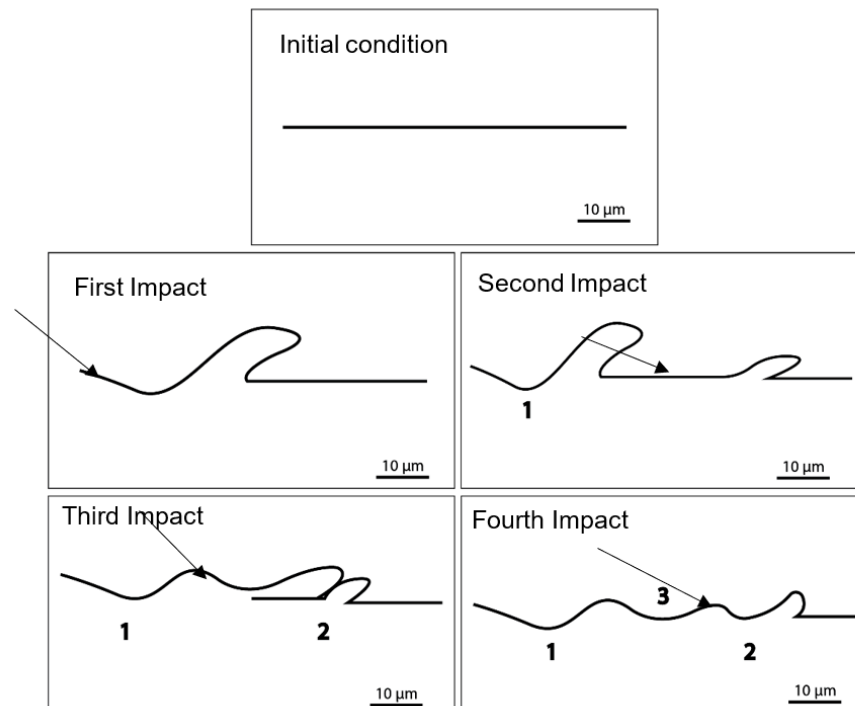
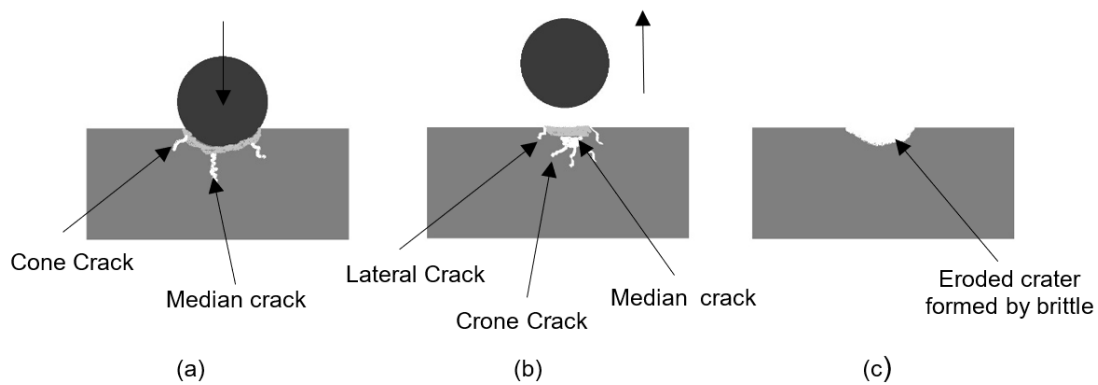


Fig. 1 - Graphics of erosion mechanism in pliant materials

Finnie suggested that microtechnology leads to the degradation of pliant materials, and offered an accurate engineering model for ductile materials [6]. When the particles hit the flexible surface, it forms a crater, and subsequent particles accumulate around the hole, increasing its effectiveness. The cascading strokes remove the material that eventually accumulates. However, the model reduces particle precipitation with a more significant impact angle than experimental data. More researchers later discussed this limitation to elaborate particle erosion mechanisms of soft materials [7]–[10].

Unlike pliant materials, the mechanism of erosion in hard particles is known as brittle materials. Erosion of brittle materials is believed to be associated with crack formation [11]. When particles hit a fragile surface, lateral, and radial cracks are formed, and the final impact on this surface leads to grow the cracks. These cracks separate the target surface into small pieces and eliminate the particles when they hit the surface. The crack formation and diffusion continue to be the primary erosive mechanism for brittle materials [12]–[14]. Fig.2 shows a diagram of the wear mechanism of brittle materials.



**Fig. 2 - Erosion mechanism in fragile materials: (a) expansion of cracks; (b) closure, and median of lateral cracks; (c) eroded crater formed**

### 2.1 Parameters in predicting solid particle erosion

The erosion mechanism of a solid is affected by several factors with simultaneous presents. In order to develop a precise erosion model or accurately predict erosion, appropriate parameters for the erosion process must be defined [15].

Several models have been proposed to predict pipeline disruption based on these criteria. In addition, Meng frequently mentioned parameters among the different erosion correlations found in the literature [16]. Nevertheless, Clarke defined the following parameters that are most important in particle collision erosion which include Particle properties (size, shape, material), particle impact velocity, particle impact angle, carrier fluid properties, target wall properties, and particle concentration, etc. [17], [18].

### 2.2 Empirical estimates of pipeline erosion

Application 14E, API RE 14E, proposed by the American Petroleum Institute [19], is one of the first empirical equations used to estimate erosion rates in the oil, and gas industry. According to Clurey, and Shirazi, this procedure demonstrates that erosion rate can be used in the absence of specific knowledge of fluid erosion [20]. In other words, the process determines the rate of production at which only an acceptable amount of wear occurs the erosion rate is determined according to the correlation given in equation (1).

$$V_e = \frac{C_1}{\sqrt{\rho_m}} \quad (1)$$

Where;  $V_e$  is the erosional velocity,  $C_1$  is an empirical constant, and  $\rho_m$  is the fluid mixture density.

The usage of this application is elaborated by its ease of use, and the lack of other methods available [22]. However, this correlation is unsuitable for systems where sand and other solids are expected to be produced. This is because it indicates that the velocity limit may be higher at lower liquid density. Meanwhile, high-density liquid sand causes more erosion than common density gases [23]. Therefore, Fixed  $C_1$  values for continuous, and intermittent operation in solids-free liquid systems are 100, and 125, respectively. API RE 14E suggests a reduction in factor C in the presence of particles, and corrosive conditions for the application of this reduction [24], [25].

Some researchers have proposed different values for C in equation (1) because the equation has shown that it is easy to use, and conservative even for clean tasks such as liquid droplets. However, for primitive services, some essential parameters, including particle size, and shape, and performance, and impact properties, were not included in the correlation.

The equation predicts a high rate of erosion as the density of the liquid mixture decreases, so it is non-physical. As the density of the fluid decreases, the drag on the particles decreases, causing the particles to collide at higher speeds, causing more erosion [26]. Due to the limitations of this erosion equation, researchers have developed more complex relationships to predict deterioration.

To comply with the limitations of the API recommendation RP14E, Salama offered a method for computing erosion damage as a function of fluid, and flow properties [27]. In addition, the authors used experimental data from Rabinowitz showing the results of erosion of ductile metals under the influence of solid particles [28].



$$ER = 1.86 \times 10^5 \frac{W_p V_f^2}{P D^2} \quad (2)$$

Where;  $ER$  is the erosion rate in mils per year,  $W_p$  is the sand flow rate in bbl/month,  $V_f$  is the fluid flow velocity,  $D$  is the pipe diameter in inches, and  $P$  is the material hardness in  $psi$ .

Erosion rate predicted using equation (2) although overestimated by a factor of 1.44, the correlation's validity was established compared to available experimental data. Results presented showed that for flow in elbows, and tees, erosion rates in tees are about 50% lower than elbows [29]. Equation (2) is therefore rewritten for taking into account variations in bends or joints in the form in equation (3);

$$ER = S_m \frac{W_p}{V_f^2} D^2 \quad (3)$$

Where  $S_m$  is a geometry constant. The values suggested for  $S_m$  are;

$S_m=0.038$  for pipe bends, and  $S_m = 0.019$  for tees.

Equation (3) anticipates erosion rate more precisely for gas flow systems, since it was evolved based on the results in the erosion data in air-sand flow.

Bourgoyne conducted an experimental study to measure erosion rate for various field conditions. The author measured erosion rate in gas-solid, liquid-solid, and mist-solid flows in diverse systems, and proposed a correlation for predicting wear rate in dry gas flows [30].

For gas continuous phase (Dry gas or mist flow);

$$ER = F_e \frac{\rho_p}{\rho_t} \frac{W_p}{A_{pipe}} \left( \frac{V_{SG}}{100\alpha_g} \right)^2 \quad (4)$$

For liquid continuous phase:

$$ER = F_e \frac{\rho_p}{\rho_t} \frac{W_p}{A_{pipe}} \left( \frac{V_{SL}}{100H_L} \right)^2 \quad (5)$$

Where;  $ER$  is the erosion rate in  $m/s$ ,  $F_e$  is the specific erosion factor,  $\rho_p$ , and  $\rho_t$  are the densities of the particle, and wall in  $kg/m^3$  respectively,  $W_p$  is the sand flow rate in  $m^3/s$ ,  $A_{pipe}$  is the cross-sectional area in  $m^2$ ,  $V_{SG}$ , and  $V_{SL}$  are the superficial gas, and liquid velocities in  $m/s$  respectively,  $\alpha_g$  is the gas volume fraction, and  $H_L$  is the liquid hold up.

Equations (4), and (5) were developed based on experimental data obtained at high Flow rates observed in diverter systems. Hence, under low concentration, their applications to oil, and gas production systems are questionable. The study reports a 29% percent error in erosion prediction, and an order of magnitude decrease was observed in the erosion rate when the elbow was changed to a tee or vortices elbow [30].

Svedeman investigated the applicability of Bourgoyne's predicting wear rate to lower flow velocities [31]. An average over prediction of 25% was observed when a comparison was made with erosion data from Weiner's experiment [32]. Because different wear mechanism has a varying controlling parameter, the authors rearranged Bourgoyne's equation. They recommended the correlation shown in equation (6) for erosion velocity for erosive service based on an acceptable wear rate of 5 mils/year.

$$V_e = K_s \frac{D}{\sqrt{W_p}} \quad (6)$$

Where  $V_e$  is the erosional velocity in  $ft/s$ ,  $D$  is the pipe diameter in inches, and  $W_p$  is the sand flow rate in  $f t^3/day$ .  $K_s$  is erosion constant obtained from Bourgoyne's specific erosion factors which depend on the flow conditions as well as material, and geometry.  $K_s$  is 1.34, and 7.04 for long radius elbows, and plugged tees correspondingly.

In this regard, Swiderman, and Arnold proposed the same ratio as Salama [31]. Therefore, erosion, which causes damages to the pipes, should be limited. In addition, criteria for determining the correct pipe size have been offered for designing a multiphase pipeline in the area where erosion is expected to happen. Therefore, various  $S_m$  values are proposed; 0.017 for prominent radius elbows, 0.0006 for plugged tees.

Jordan offered a new method to calculate erosion for multiphase oil and gas pipelines. It is suggested that the rate of physical volume loss should be proportional to the square of the particle velocity, and proportionate to the volume rate of the target wall at which the target wall collides with the particles [3]. Results correlation equation is presented in equation (7).

$$ER = 10^{C_1} V_{SG}^{2.349} W_p^{0.9535} \left(1 - \left(1 + \frac{1}{2r_c}\right)^{-2}\right)^{\frac{1.8885}{2}} \quad (7)$$

Where  $r_c$  is the bend radius of curvature. The parameters also have similar units as to the equation of Bourgoyne.  $C_1$  is equal to -4.9619, and -5.4355 for the cast, and unseamed materials correspondingly.

Salama carried out a study to investigate the basis of the recommendations of API RP14E, and the authors found out that alternative approaches have been proposed for establishing erosional velocity in particle-laden flows [27], [29]. But none of these have been put to use due to their complexity. Based on the findings, the author proposed a new simplified model for erosional velocity in particle-laden fluids (equation (8)). This unique correlation incorporates pipe diameter, fluid density, and sand flow rate in the previously developed correlation by Salama, but the influence of elbow radius of curvature was not considered. The results did not show any substantial difference between erosion rates in elbows with a radius of curvatures (RC) of 1.5, and 5. The equation is also applicable to multiphase flow.

$$ER = \frac{1}{S_m} \frac{W_p V_m^2 d_p}{D^2 \rho_m} \quad (8)$$

Where;  $ER$ ,  $W_p$ , and  $D$  are in mm/year, kg/day, and mm respectively.  $d_p$  is the particle diameter in microns,  $V_m$  is the mixture velocity in m/s, and  $\rho_m$  is the density of the fluid mixture in kg/m<sup>3</sup>.  $S_m$  is a geometry-dependent constant. Empirical erosion equations are easy to use but can only be applied to operating conditions similar to the experimental conditions for which they have been developed [33]. Still, the erosion mechanism could change with the slightest change in conditions. Due to this, researchers developed mechanistic models to aid erosion prediction in a comprehensive, and complex scenario. Although mechanical models incorporate various parameters that could influence the erosion phenomenon, they were evolved reliant on the physics, and mechanisms of erosion [11].

### 2.3 Mechanistic erosion prediction

Shirazi offered preliminary guidelines for addressing shortcomings of API RP14E [25]. The instruction manual only covers the steps for estimating the characteristic velocity, and particle size below minimum wear. The model considers the influence of several variables on erosion rates, such as grain size, flow shape, pipe size, material type, sand density, sand intensity, speed flow, viscosity, liquid density, etc. In this procedure, it is assumed that if the geometry collides just before impact, the particles must reach a liquid layer called the suspension zone; Similar static length concepts have been introduced to describe the effects of geometrical shapes, and masses (Fig.3) [13], [34].

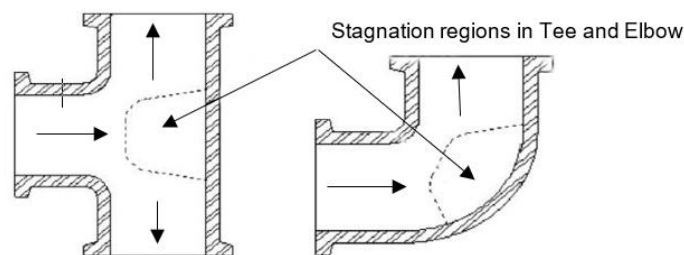


Fig. 3 - Stagnation zone in tee, and bend

Depending on the type of geometry, the stagnation length is obtained from Equation (9) or Equation (10).

For elbows, the length of the region of stagnation is obtained from;

$$\frac{L_{stag}}{L_{ref}} = 1 - 1.27 \tan^{-1}(1.01D^{-1.89}) + D^{0.129} \quad (9)$$

For tees, the length of the region of stagnation is obtained from;

$$\frac{L_{stag}}{L_{ref}} = 1.35 - 1.32 \tan^{-1}(1.63D^{-2.96}) + D^{0.247} \quad (10)$$



Where  $D$  is the pipe diameter,  $L_{stag}$  is the length of a stagnation region, and  $L_{ref}$  is the reference length (1.18, and 1.06 inches for elbows, and tees respectively). For small pipe diameters,  $L_{stag}$  is a firm function of pipe diameter while for pipe diameters more than about 6 inches, pipe diameter has little influence on  $L_{stag}$  [11]. Flow velocity is calculated from Equation (11). The characteristics velocity of the flow is equal to the mean velocity of the flow.

$$V_f = V_{char} \left(1 - \frac{x}{L_{stag}}\right) \quad (11)$$

Where  $V_f$  is the fluid velocity, and  $V_{char}$  is the flow characteristic velocity. The particle impact velocity is obtained by solving the particle equation of motion as shown in:

$$m_p V_p \frac{dV_p}{dX} = 0.5 \rho_f (V_f - V_p) |V_f - V_p| C_D \frac{\pi d_p^2}{4} \quad (12)$$

Where  $m_p$  is the particle mass,  $V_p$  is the velocity of the particle,  $V_f$  is the velocity of the fluid at the particle position,  $\rho_f$  is the density of the fluid, and  $C_D$  is the drag coefficient. As an initial boundary condition, the particle equation of movement requires the particle velocity ( $V_p$ ) at  $X = 0$ . primary particle velocity is also presumed to be the same as  $V_{char}$ . Tracking of a particle is ceased, and velocity at that position is pondered as the effect velocity when the distance between the particle, and the wall equals the particle radius. The drag coefficient is expressed as:

$$C_d = \frac{24}{Re_p} + 0.5 \quad (13)$$

where  $Re_p$  is the particle Reynolds number, and it is expressed as:

$$Re_p = \frac{\rho |V_f - V_p| d_p}{\mu_f} \quad (14)$$

$\mu_f$  is the fluid viscosity.

The erosion ratio is finally obtained from equation (15).

$$ER = 1.73 \times 10^{-6} V_L^{1.632} \quad (15)$$

Where  $ER$  is the erosion ratio of the mass of the objective material removed to the mass of a particle, and  $V_L$  is the particle impact velocity. The impact velocity of the particle,  $V_L$ , is calculated from a simple 1-D particle tracking mean along the stagnation length.

Equation (15) is generated based on damping data for low carbon steel. The results showed that the critical velocity of a single-layer liquid is higher than that of the gas [35]. However, this procedure presumes that the particle's path is straight, and does not consider the effect of the turbulence on the particle's path. Developed initially for single-phase control, this model was later extended by McLaury, and Shirazi stages, forming the basis for many later mechanical models [20]. In addition, Mazumder developed an automated model that takes into account the characteristics, and behavior of multistage gas, and liquid phases [36].

We observed that the model predicts erosion by calculating the collision velocity of particles based on one-way particle tracking. This limits its application to flow conditions where particles of sand or gas in the range 50-100  $\mu\text{m}$  are used as the carrier liquid. The collision rate of diamond particles and their chaotic nature have been shown to affect erosion prediction significantly. He proposed a 2D mechanical approach to capture the properties of these particles. This process consists of three main steps. First, 2D flow field data were obtained from the static field centers and a CFD simulation of the flow center. Second, the stream field receives the data to calculate velocity, angle, and collision position. Unlike 1-D, which tracks a representative particle, a 2D model follows multiple particles. Finally, information on the effect was added to the etching equation developed by Zhang [23] to explain the impact of particle collision velocity, and turbulence. The 2D model provides more representative information about the collisions of particles and significantly improves the etching behavior in the 1D model. These are important for growth fluids that carry fine sand particles.

Arabinejad created the almost mechanical model for predicting the degradation of various objective materials by solid particles [37]. This model is based on experimental data from direct collision tests taking into account the properties of the target particles, and materials, and suggests two different

Taheri Fard, A.

Pipe erosion under multiphase flow. A review;

2021; *AlfaBuild*; Volume 19 Article No 1901. doi: 10.57728/ALF.19.1



mechanisms involved in the decomposition of the particles. Hence, the erosion equation has two parts: erosion, and shear deformation. The particle's velocity is calculated by particle image velocity (PIV) measurement, and the model's predictions are compared with different confirmation conditions. The correlation shows that the collision angle of particles depends on the size, and velocity of the particles.

Parsi discovered a correlation of reliable erosion estimates in sand, and gas flow conditions. This approach consists of three steps. First, the proportional analysis is performed to obtain unreachable combinations, such as Reynolds number, diameter ratio, and density ratio, particle flow correction, and knee motion. Second, a study of the effect of the target wall material on erosion was conducted, and finally, experimental factors were correlated to take into account sand particle size [38].

Correlation is an effective tool for estimating erosion in gas conditions, and airflow with minimal design effort. The use of correlations is consistent with experimental data. However, it was developed on a limited experimental database and took all particle, and flow parameters into account.

Erosion is difficult to predict even in single-phase flows, and this complexity dramatically increases due to the nature of the formation of multiphase flows. The flow of polyphases makes it challenging to detect particles. In a multistage flow, the liquid, and gaseous phases' spatial distribution, and velocities are constantly changing [39].

McLaurie, and Shirazi have developed a mechanical model for predicting knee, and skin wear rates, and advanced impact technology [23]. They extended multistage flow conditions. The newly developed model takes into account many physical variables such as fixed flow rate, mixed viscosity, particle impact rate, pipe diameter, liquid density, curvature radius. In this model, the thickness, and viscosity of the liquid are calculated from its constant length as a function of the fluid, and gas volume as a function of the flow condition. It was found that when there was movement between the liquid and the particles, the particles weakened because there was more knee wear, and the particles could not be directed as they passed. Consequently, the factors that increase the gearshift slow speed erode. Comparing the results with API 14RE recommendation data, we found that the test procedure is very conservative at high fluid flow rates.

Mazumdar has proposed a mechanical model to prefigure sand erosion in multiphase flows under the chute. The effect of particle velocity on erosion rate in gas and liquid stream has been studied. This model uses a unique correlation proposed by Ishii, and Mishima to accurately calculate the single liquid fraction of the gas core under a variety of flow conditions. It was found that the velocity of the droplets had a significant effect on the momentum of the particles, causing tremendous erosion [40]. Therefore, it is advisable to carefully evaluate the droplets to determine the sand grain's velocity before reaching the stationary zone. The particles are also captured by the droplets moving at the same speed as the gas. These particles have a more significant corrosive destructive effect than the particles in the liquid film that slowly move closer to the tube wall. Despite these biases, the predicted erosion provides a reasonable estimate of the erosion resistance of multiphase compared to the data obtained from erosion tests performed on multiphase clones. The authors also found that erosion damage was significantly more significant in vertical circulation at high gas and liquid velocities. The model's predictions are 2.9 to 6.8 times higher at fluid flow, and 4.2 to 8.2 times higher at the flow rate than experimental data. Predictions for bubbles, fungi, and erosion are in multiple stages higher, and more conservative than practical. Based on this, we recommend validating your model, and optimizing further [41]–[44].

In addition, Zhang offered a two-dimensional mechanical model to predict sand erosion in slug flow. All previous automatic models were based on a one-way approach. The bidirectional system has been extended to overcome multistage flow erosion problems. In this model, it is presumed that the particles are evenly disseminated in the liquid phase, and do not promote erosion due to their slow velocity. The body of the bullet also appears as a representative phase. The wear rate is estimated to be successful at different points in the shape of the knee. The forecast data is located on a slope at  $45^\circ$  with a perfect sense of the available information, but at  $90^\circ$ , the forecast is more fragmented. This is due to the influence of secondary circulation in the elbow joint. The 2D method is usually more accurate than the 1D method [45].

Shirazi developed a semi-mechanical model to estimate sand erosion degree during multistage gas formation, and flow. Unlike API RP 14E, this form can be used in two ways. One is to provide the maximum permeability rate for a particular work environment. The other can be used to determine the surface velocity of liquids, and gases if a maximum permissible permeability rate is specified [46]. This model significantly improves the previous mechanical model with a dense pressurized gas with a fine particle stream in the liquid stream. It also applies to situations in one state to interpret the effects of various parameters such as particle diameter, and size, fluid density, and viscosity, flow rate.

Taheri Fard, A.

Pipe erosion under multiphase flow. A review;

2021; *AlfaBuild*; Volume 19 Article No 1901. doi: 10.57728/ALF.19.1



Recently, Kang and Liu have developed a mathematical model that predicts the erosion of solid particles at the symmetrical knee plane of a circular flow. The model tracks the particles as they collide with the tube wall, and takes into account the particle's movement in both the gas core and the liquid membrane. In this model, it is assumed that the gas core flows evenly and that the velocity, and thickness of the liquid film when bending the tube are the same. The length of the inlet should be sufficient to mix the particles with the carrier prior to bending. Kang also investigated the effect of various macroscopic factors on prevalence. The model's accuracy is low at low speeds, and low throttle but high at high speeds. The results show that the permeability rate increases with increasing particle size, and surface gas velocity.

Nonetheless, the impact of a liquid's surface velocity on the degree of wear depends on the liquid filling condition. The results presented show that the mean deviation from the available experimental data is 26.15%. However, this model cannot provide more reliable information about the flow field and is limited to cyclic flow. Kang and Liu developed a probability model to predict the wear of a periodic sand generation. The authors calculated erosion caused by a group of grains of sand by calculating erosion damage caused by one grain. Probability models for first and second collisions are based on Liu's experiment. The results presented are in good agreement with the recirculating system data. The authors concluded that the second particle collision has a considerable effect on the size, and location of the erosion under toroidal flow conditions. However, its application for other multistage diagrams is still under discussion [47]–[49].

### 3 Experimental analysis of sand erosion in pipelines

Mazumdar conducted an experimental study to determine the maximum damage caused by adsorption erosion in single-phase, and multiphase transverse, and longitudinal currents. He used a resistance sensor for more accurate thickness loss measurements because of a low-density, corroded aluminum bend pattern. Single-phase erosion tests were performed at a gas-surface velocity of 34.1 m/s in a vertical flow, a gas-surface velocity in a polyphase flow, and a liquid velocity of 33.5, 27, 4, 18.9 9.8 m/s. 0.03, and 0.3 m/s longitudinal and horizontal pipes. The results show maximum thickness loss at 42.5  $\mu\text{m}$  at 55° from the inlet for single-phase, and polyphase currents at gas-surface velocities of 9.8, 27.4, and 34.1 m/s the average thickness loss. Concentric loss increases because the gas velocity increases at the same rate as the surface liquid. In addition, with a multistage flow, the most significant thickness losses are observed between 55°, 35°, and 55° in the vertical, and horizontal pipes [41], [50]. Graham Measured the intermittent current erosion by coordinate the measuring machine (CMM). The pipeline network is 53 mm in diameter, and the pilot station is designed to allow vertical flow. The elbows are also aluminum blocks. Most traces of wear are seen near the elbow. The CMM results were comparable in quality versus simulation, and visualization with good consensus [51], [52].

Kesana applied a new non-invasive ultrasound to measure erosion at 16 different positions in a normal knee. The experiment was first performed using a one-step vector (gas sand) and was then extended to multiphase flow conditions. The effects of particle size and liquid viscosity have been studied, and the results show an acceptable agreement with the accessible experimental data. In experiments using ultrasonic technology (UT), corrosive substances are measured with an intrusion resistance (ER) sensor in the straight section of the tube. Curved erosion patterns have been successfully determined, and maximum abrasion air sand flows are observed at about 45°. Still, under multiphase conditions, erosion is kept at the top of the turn, which also increases with ten cp viscous fluids due to increasing particle size. Nevertheless, erosion increases slightly from 1 cp but decreases after viscosity increases by 40 cp. The results of the ultrasonic sensor (UT), and electrical impedance (ER) are similar.

Kesana experimented with a gas-surface velocity between 9.1 m/s, and 35 m/s, and studied sand erosion in a multistage slag flow between 0.76 m/s, and fluid velocity. He used three fluids with viscosities of 1 cp, ten cp, and 40 cp. The test section consists of a standard 76.2 mm elbow. The authors found that the total error of spider particles in the well-ventilated stopper was inferior to that of the slag flow system. The simulated cork mixing area ran on lower shale and pseudo-grain. As a result of the disturbance, the particles can float over the entire cross-section of the pipe in the so-called slab form, resulting in some of the particles falling on the wall of the tube. It is called the impurity-drainage system. Kesana extended a similar procedure to investigate the impacts of particle size, and fluid viscosity on the cyclic, and directed flow. Three various sand sizes (20, 150, 300  $\mu\text{m}$ ) are used in the test. A resistance sensor (ER) is used to measure the erosion, and curvature directly of the pipe following measurements of 45°, and 90° vertical, and inclined cross-sections show that large particles cause more erosion under

Taheri Fard, A.

Pipe erosion under multiphase flow. A review;

2021; *AlfaBuild*; Volume 19 Article No 1901. doi: 10.57728/ALF.19.1





all operating conditions than small particles and the effect of particle size on erosion. The erosion rate of a toroidal stream is higher than the pellet stream, regardless of the state or fluidity of the liquid.

In the case of a grain flow, the particles move inside the liquid pellet due to the sand, causing polishing damage to the pipe located in the circulating flow in the low-density zone of the gas core [26], [53]–[55].

Parsi also measured erosion of gas-dominated multilayer sand grains in the riser by ultrasonic method (UT), and obtained results from Kesana, and compared with the erosion data obtained [11]. The test is performed with a standard vertical elbow (VH) made of stainless steel and has an inner diameter of 76.2 mm. Erosion rate, the effects of surface velocity, particle size, gas, and liquid viscosity are measured.

In addition, the erosion rate was checked using sand grains of 20, 150, and 300  $\mu\text{m}$  which the liquid viscosity is one cp, and ten cp, and low gas velocities ranged from 9.8 to 49 m/s, and fluid surface velocity ranged from 0.1 to 0.55 m/s. Practically, the erosion rate of the vertical, and horizontal inversion is measured vertically, and horizontally in all flow conditions. The results also show that changing the velocity of the liquid surface does not affect the erosion rate. This is because the flow system does not change, and the inlet of the elbow is greater than  $45^\circ$  when mixing the charge.

Vieira used a resistance sensor to measure the constant erosion of a circular multiphase flow; his study focuses on collecting experimental data for large multistage currents with constant curvature of 76.6 mm. The reduction in gas velocities ranged from 11 m/s, 48 m/s, 0.004 m/s, and 0.27 m/s, using the viscosity of 1 cp, and ten cp, and three different sand sizes (20, 150, 300  $\mu\text{m}$ ). In addition, he studied the effects of ER sensor position, flow direction, sand mass, flow rate, and liquid viscosity. They found that converting the carrying fluid from gaseous sand to a low flow coil stream reduced the longitudinal wear of the knee four times. Increasing the viscosity of liquids around the slope also minimizes the effect of the particles on the walls.

Additionally, a significant metal loss is recorded with a  $45^\circ$  probe regardless of operating conditions. In the horizontal direction, the liquid film condenses at the bottom of the tube, reducing erosion. Vieira has investigated the effects of particle size, and velocity of the gas, and liquid on the erosion speed, and properties. The authors have used non-contact ultrasonic measurements in place of resistance sensors to analyze erosion under multiphase cyclic flow conditions with longitudinal, and transverse curves. At higher gas surface velocities, erosion is first reduced and then increased again after reaching a minimum. However, it is often observed that erosion increases with increasing particle size, and airflow [55], [56].

## 4 CFD modeling of pipe erosion

### 4.1 CFD modeling of pipe erosion in single-phase flows

Zhang investigated erosion forecasts using CFDs. The authors studied the particle's motion in the vicinity of the wall. They compared the calculated model of solid particles with experimental data to ensure the model's accuracy in calculating the displacement particles. The effect of the turbulence coil on the area near the wall was examined, and its impact on the collision velocity of the particles was also studied. Comparisons are made by applying conventional wall features to monitor wall particles and reflect wall particles. The flow is modeled by solving equations of continuity, and momentum. The orbits of the particles use a different topology (DPM) model for integrating force balance on the particle, and the effect of turbulence on it. The movement of particles is considered using a Discrete Random Walk (DRW) model. The areas near the wall were solved using the RSM noise model with standard wall functions, and the erosion was calculated using the method of Zhang. The expected effects of grain abrasion, and disturbances before, and after wall reorientation were applied, showing changes that significantly impact erosion results compared to experimental data. Periodic calculations were observed for the turbulence of a standard  $90^\circ$  rotation to avoid non-cyclical effects, and reduce multiple shocks of small particles (25  $\mu\text{m}$ ) caused by turbulence.

Using the standard wall function in the wall trace reduces the estimated wear of large particles by small amounts, and the estimated wear of small particles twice. Erosion results of small particles were more suitable. Zhang also performed a numerical study to find out maximum wear on the elbow. At a knee height of about 0.628 m, and a diameter of 0.1 m, he studied the effects of the suspension speed, bending direction, and bending angle. The particle path and interaction between particles are calculated using a separate element model, and the liquid properties are constructed using the Reynolds mean Navier-Stokes equation. It was found that the cutting speed and maximum wear conditions affect the areas damaged by the increased shearing force. The bend direction also significantly affects the erosive

Taheri Fard, A.

Pipe erosion under multiphase flow. A review;

2021; *AlfaBuild*; Volume 19 Article No 1901. doi: 10.57728/ALF.19.1



damage to the upper pipe or the vertical pipe when the particles settle to the bottom of the upper pipe, and most of the particles move away from the central shaft [23]. In U-shaped pipe, the largest wear surface is observed with two different spikes. Due to gravity, it appears above the knee at about  $43^\circ$ ,  $90^\circ$ , and  $160^\circ$  [58]. Results are compared with previous studies with a tube 30 cm in diameter, and 100 cm in length [59]. The gas-phase was simulated by solving the Reynolds averaged Navier-Stokes equation (RANS) with the standard  $k-\epsilon$  model, and the particles were monitored by different element methods (DEM).

The turbulence distribution was calculated using the random turbulence sheet (DRW) model. The sizes of sand grains used are 100, and 200  $\mu\text{m}$ . The results showed that the erosion rate of the inner, and outer walls increased as the roughness of the border grew, and the erosion rate was much higher than that of flat walls, regardless of the grain size of the wall. As the roughness increases, the concentration of particles near the inner border of the bearing increases, making it easier for the particles to hit the wall, and speed up abrasion. The authors also noted that the outer wall of the bent tube is more abrasive than that of a conventional round pipe with the same outside diameter and that the wear rate increases as the radius increases.

Chen proposed the CFD-DEM two-step erosion protection method for pipe elbows. Interaction of liquid particles is considered. Using water as a continuous phase, he estimated the velocity, and position of sand grains 150  $\mu\text{m}$  in diameter, and maximum erosion with diameters of 90, 60, 45, and 40 mm. The continuous phase is modeled by solving the Reynolds Navier-Stokes equation. The standard  $k-\epsilon$  model considers the turbulence of the curling current, and the interaction with the single element model (DEM), taking into account the motion of grains of sand, and liquid particles. The maximum wear rate varies for the three knees, and the  $90^\circ$  knee is arguably the most wearable-entire wearing area at or near the elbow. Chen also recommends replacing wide-angle elbows, such as low angles ( $45^\circ$ , and  $60^\circ$ ), to reduce erosion [60].

Zahedi carried out the marginal erosion analysis is performed with a large radius, typically  $90^\circ$  ( $r/D = 1.5$ ). In order to analyze the effect of particle size, fluid velocity, pipe diameter, and radius on maximum gas, and sand erosion. The inside diameters tested are 2, 3, and 6 inches, and the gas surface velocity ranges from 11 to 27 m/s. Erosion level was calculated using a correlation developed by Vieira for the Erosion / Erosion Research Center (E/CRC), and the backflow of the grain was masked using model Grant, and Tabkoff [61]–[63]. The results are in a cordial relation with the experimental data of Vieira. For single-stage gas, and sand flows under low-pressure conditions, the most vigorous erosion is observed at an inclination of about  $45^\circ$ . It was found that 300  $\mu\text{m}$  particles caused double erosion of 150  $\mu\text{m}$  particles. Increasing the surface gas speed also increases the erosion rate. Still, due to the increased pipe diameter, and the properties of the particles, the erosion rate decreases significantly under constant flow conditions. Maximum wear of ample radius curves is also less than at standard angles.

Mahdavi studied erosion on slurries. The authors studied the effect of particle size and velocity on sand erosion rate at different concentrations. The penetration rate of the liquid is set at 45 ft/s, and sand concentrations of 1, 6, 10, and 15% are used with a grain size of 300  $\mu\text{m}$ . The flow solution was derived by resolving the Reynolds Navier-Stokes equation (RANS) using the Euler method. The particles were monitored to compare the hysteresis area, and particle plot results and the calculation of Erosion coefficient math was performed using the performance correlation of Vieira's experiment.

The Euler-Granular approach reduces experimental data, but erosion estimates decrease slightly as sand content increases, according to the Euler-Granular diagram. Still, in the case of Euler-Lagrange, other sand is erosive. It was also found that increasing sand content resulted in an increased mineral loss.

In all studied cases, the concentration, and depth of erosion can affect the fluid flow, and change the path of the particles. Therefore, it is concluded that the difference between the results of these two approaches is related to the two-way interaction of particles, and liquids in the Euler particle method [64].

Xu studied a numerical analysis of the particle concentration, friction modulus, rebound modulus, and spring stiffness modulus on knee wear was performed, and the results compared with the existing data. To calculate the flow physics, two-dimensional CFD-DEM simulations were performed. The motion of the particles was calculated by the discrete element method (DEM), and the average value of the flow field from Navier-Stokes to Reynolds. Erosion rate was calculated using a grain scale erosion model based on the direct impact studies of Ashrafizadeh [65]. The tube has a diameter of 25.4 mm, a vertical length of 1200 mm with a standard inclination of 90 degrees, the friction of 0.1 to 0.6, and a particle diameter of 150  $\mu\text{m}$ . The entry speed is 45.72 m/s, and the recovery coefficient is four times between 0.8 to 0.95.

Taheri Fard, A.

Pipe erosion under multiphase flow. A review;

2021; *AlfaBuild*; Volume 19 Article No 1901. doi: 10.57728/ALF.19.1



The mass currents in the study were used as 0.000208, 0.00208, 0.0208, and 0.208 kg/s. As a result, it was indicated that the particle concentration played a major role in flexural erosion in increasing the grain flow, which proportionally increases internal wall erosion of the elbows significantly. Finally, it was found that friction coefficient, rebound coefficient, and spring stiffness have minimal influence on knee wear [66].

Peng and Cao studied the numerical velocity to study the solid erosion of liquid, and steel pipe curves, and at the same time, survey the bending velocity, and direction of the flow [67]. The author identified five general correlations and selected the most accurate correlation in this study. Peng also analyzed the relationship between Navier-Stokes number and maximum erosion. It was found that all erosion equations gave the same erosion pattern, but no significant differences were observed in his studies [68].

Al-Khayat developed a 3D-CFD model to study various factors affecting tube wall erosion during the transport of coarse sand [69]. This model delineates the turbulent transport of sand particles using different crude oil transport parameters such as viscosity, density, velocity, and temperature.

Particle motion was monitored using the Discrete Phase Model (DPM). The pipe and sand diameters are 0.2 m, and 170  $\mu\text{m}$ , respectively, and the flow velocity is set at 0.3 m/s. The results obtained show agreeable relation with the available experimental data. An increase in erosion is observed as the friction between the oil, and the pipe wall increases. When viscosity increases from 1MPa to 20MPa, the erosion rate increases by almost 100%, so the oil's viscosity has a significant effect on the erosion rate. However, changes in the sand's abrasion rate, oil density, temperature, and mass flow are not dependent on it [70].

#### 4.2 CFD modeling of pipe erosion in multiphase flows

Due to the complex interactions between multiphase flows, and particles, many scientists now use computational fluid dynamics (CFD) to predict and analyze erosion. CFD has the advantage of being able to indicate erosion rates, maximum wear points, and identify potential leaks, and erosion times. It can also be used for complex geometries and complex fluids.

Peng Jr developed CFD abrasion evaluation and compared results of the rusting equation for CFD symbols using empirical equations. He designed 1-inch stainless steel 316 with a Brinell hardness of 230 BHN. The carrier liquid is a mixture of water, and air in a flow system with velocities on the surface of the liquid, and gas at 34.1376 m/s, and 0.3048 m/s, correspondingly. The grains of sand have a diameter of 150  $\mu\text{m}$ , and a mass of 0.006 kg/s (shear stress transfer) flow modeled by multiphase using the Euler method, and particles monitored by the Lagrangian system. The erosion rate was calculated using commercially available CFD package equations proposed by Erosion Finnie and compared with the experimental correlation results developed by Salman (1998), DNV (2007). The results showed a good agreement on erosion rate, and Salama et al. (2000), and DNV (2007). However, if the fluid flow decreases from horizontal to vertical (H-VD), the erosion rate will be at least 20 times higher [29], [71].

Nguyen conducted experimental collaborative studies to determine how the surface development of substances due to erosion affects the erosion mechanism of the mixed flow of water, and sand. A stream of water and sand was prepared according to the Euler-Lagrange method. Water is considered a continuous phase guided by the Navier-Stokes equation and another sand grain of the Lagrange phase. In addition, k noise was recorded using the k- $\omega$  model, and the buoyancy rate of the particles passing through the wall was determined by the carrier model [23]. The rate and nature of erosion were evaluated by the method of Oka [72], [73]. Using the surface configurations obtained after 5, 15, and 30 minutes of experience, an engineering model to simulate the number of direct collisions of particles was generated. The erosion rate was found to be highest in the section formed after 15 minutes due to the sheer force, and the impact rate of the particles was higher than the cutting rate at this time. Therefore, the minimum erosion rate is indicated on the surface profile after 30 minutes. From experimental data, and numerical results, it can be seen that the direction of the erosion rate is the same, both linearly dependent on the collision speed. Increased impact speed increases erosion speed. However, for the same flow rate, the numerical model slows down the erosion rate compared to the experiment. This is probably due to the effects of the particle interactions that have not been recorded in the simulation [74], [75].

#### 4.3 Erosion Modeling in Elbows Mounted in Series

Most researches have focused on sufficient length following particle erosion for simple convex geometry, and flow development. However, recent oil and gas flow under extreme conditions has



required more complex piping systems with line installations, but with detailed calculations of in-situ erosion data, which requires a better understanding of grain erosion under these conditions.

Deng experimented with four bends (vertical-horizontal, horizontal-horizontal, horizontal-vertical, horizontal-vertical) to find the puncture points in the air transmission system that is strongly affected by the direction of rotation. Air is used as the carrier fluid, and high concentration olivine sand is used for the particles. A steel pipe with an outer diameter of 60.3 mm, wall thickness of 3.9 mm, and an average particle size of 294  $\mu\text{m}$  is used. The results showed that the starting point position was most affected by the direction of curvature due to the smooth distribution of particles, and the distribution of the flow. Furthermore, the downward vertical, and horizontal elbows have the shortest drilling life, and the deepest penetration point at about  $25^\circ$ .

In comparison, the upright horizontal, and vertical elbows are drilled closer to the drill point by about  $8^\circ$ . Thus, its lifespan is slightly longer than when bent and bent down of the tube, but there is no significant difference in the position of the puncture point in the other curvature directions. However, the minimum distance between two consecutive elbows in the used current path is 300 times the pipe diameter, so any interaction currents between straight elbows are ignored [76].

Zhang focused on finding a puncture site in a tube by converting a studied core numerically into a U-shaped bend with a large radius number. The suspension speed is 18 m/s which is not affected by gravity. He solved the Reynolds averaged Navier-Stokes equation to calculate the fluid flow in order to track the particles by the discrete element method. The result shows that the leading position in terms of erosion at the first rotation angle occurs at  $43^\circ$ , and  $160^\circ$  at the second angle due to the average gravity of the curve, which causes the direct collision of particles in the first tube. Furthermore, he found that while applying the middle stage, the erosion location in the first knee is similar to the position in the normal knee by an angle of  $90^\circ$  [58].

Sedrez performed a CFD simulation of the diluted solid, liquid gas stream to determine the largest corrosive site in S-bend. The liquid was treated with medieval solution Navier-Stokes, the particles in the system. The second phase model (DPM) is calculated using an erosion model applied by ANSYS Fluent. Results for 50, and 200  $\mu\text{m}$  sand particles are displayed at three different water and air-surface speeds. The inlet gas velocities are set at 15.24, 30.48, and 45.72 m/s, and the velocity of the liquid is at 0.1, 1.0, and 10.0 m/s. At  $43^\circ$ , and  $161.3^\circ$  bending, it is  $1^\circ$  at  $20^\circ$ ,  $50^\circ$ , and  $V_{\text{sg}}$  at 15.24 m/s, the maximum erosion conditions at the inlet are  $20^\circ$ , and  $145^\circ$  at the elbow [77].

The elbow distance is 6 pipe diameters ( $L = 6D$ ). Erosion tests are performed using ultrasonic wall thickness measurements under liquid sand conditions, liquefied gas, and sand flow. The erosion test portion of the test plant consists of a tube of 50.8 mm, and grains of sand with an average diameter of 300  $\mu\text{m}$ . In CFD simulation, the RSM model, and constant field current solve the average Navier-Stokes equation (RANS) to capture the turbulence, and the particles are followed up with the model. Erosion was calculated using the correlation suggested by Arbanzad [37]. For single-phase analysis, the water velocity is 6.3 m/s, and for polyphase analysis, the surface velocities of water, and air are 5.3, and 10 m/s, respectively. The authors only present the results of position two and the erosion that was observed in the experiment. The flow of liquid sand takes approximately 16 minutes, and the removal of liquid sand-gas from large materials takes 3 minutes to sink. However, the wear styles are very similar, in both cases around  $90^\circ$  from the outer radius of the knee. It was also found that the erosion rate of the multiphase flow was 7.8 times more. In CFD analysis, the authors observed similar erosive structures in multiphase, and liquid sand flows compared with the experiments but found that erosion was more common in the second zigzag line of the multiphase stream. The maximum relative abrasion coefficient of the liquid sand stream is more than 60% [78].

Asgarpur et al. (2017) also conducted numerical, and experimental studies of continuous knee wear to study second-generation erosion. The test consists of two 10 (10D) diameter tubes and a 4-inch elbow. The test was performed under one-step, and two-step conditions and the diameter of the grain used was 300  $\mu\text{m}$ .

In the multistage test, the constant gas velocities are 31 m/s (all within the spherical flow range), and the fluid velocities are 0.016, 0.02, 0.055, and 0.1 m/s, considered in the Reynolds stress model. The sand particles were monitored using a second phase model (DPM), and a second random model taking into account the distribution of the particles in the wall. Erosion was calculated using the correlation suggested by Arbanzad. The wall material is 316 stainless steel, which dramatically reduces the erosion rate of single-phase reducers from 31 to 15 m/s, and is consumed most in the first, and second cycles. In addition, the maximum erosion range for all gas velocities is at an angle of  $45^\circ$  from the outer inlet of the first rotation when the position changes during the second rotation. In addition, based on his

Taheri Fard, A.

Pipe erosion under multiphase flow. A review;

2021; *AlfaBuild*; Volume 19 Article No 1901. doi: 10.57728/ALF.19.1



experimental results, the author found that the location of maximum erosion was the same in the first, and second rings of one-phase, and second-stage flow, but maximum erosion was larger than in one period.

Moreover, flow is greater than the flow of a gas or liquid. Erosion rate estimated by CFD analysis at 23 m/s gas velocity, well suited to single-stage test results, up to 25%, and 24% for bars 1, and 2. The abrasion position of the maximum on the first bend was well assessed but not precisely determined for the second [79].

Farokhipour modeled the amount of erosion of sand particles in the return of the two-phase gas molecular stream; the author estimates the erosion rate with four different vertical curves. Tight, constant ( $R/D = 1.5$ ), large radius ( $R/D = 3$ ),  $180^\circ$  bend were studied. The distance between the elbows is 20D. The degree of erosion was calculated by the Oka-Model method. The continuous gas phase was determined using the  $k-\omega$  SST, and RANS reject model formulas and a discrete random walk model used in DPM. Sand particles were monitored, and the particle distribution is taken into account. Sand particles 150, and 300  $\mu\text{m}$  in diameter are taken into account. The seed flow rate is also variable (1, 3, 5, 10, 15, 20 kg/day). Constant fluid velocity at 20 m/s. The  $180^\circ$  knee has better wear properties than other shapes, with 67%, 64%, and 52% lower wear rates than the acute, normal, and long knee. However, in all the cases studied, the erosion rate is proportional to the mass flow of the particles, but the  $180^\circ$  pipe curve is less sensitive to the increased mass flow of the particles, and the excitation. Three hundred  $\mu\text{m}$  is one-third of the standard arm. Similar erosion patterns have been reported due to grain size [80].

Recently, Cedrez tested the erosion in ANSYS fluent. A mixture from the multipage Euler model to discrete, and rejected models was used to predict flow erosion with tensed Reynolds. He calculated the perturbations of the system using the perturbation model and the standard functions of the wall. In addition, he took into account the drift laws of spherical, and non-spherical particles in the Langerin particle monitoring system.

The pipe diameter used in the standard elbow is 50.8 mm ( $R/D = 1.5$ ), the distance between the elbows is three diameters (3D), and the front length of the first elbow is 42 diameters (42 D). Erosion was also analyzed for two different-sized bubbles, 0.01 mm, and 1 mm. The liquid and gas velocities are 6.31 m/s, and 5.46 m/s; respectively, the particle size is 300  $\mu\text{m}$ . Their results showed that the Euler model did not take into account the secondary particle monitoring steps. Still, the experimental data showed that the secondary erosion results were better than that of the first model. Maximum erosion is evaluated by both spherical, and aspherical traction. More significant wear is also observed in the second, and first-generation compared to the test data -1 mm bubble size for best liquid separation results. The highest erosion rate was much higher than the experimental data obtained using Arabnejad's products. The erosion of the first, and second arcs increased by 37%, and 70%, respectively. Maximum wear is observed at  $88^\circ$  after starting the first, and second turn, similar to  $90^\circ$  observed in the experiment. DNV model (2007) reduced ring one, and ring wear by 26%, and 22%, respectively. In all studied cases, bend two is weaker than bend 2 [78].

## 5 Conclusions

Consequently, an extensive literature review revealed that most CFD studies on pipeline erosion use the Euler-Lagrange method to focus on continuous single-phase flow conditions. Nonetheless, erosion in multiphase flow is studied using different techniques for turbulence modeling, and other interface parameters. The double equation scrambling model has been used in erosion prediction over several years due to the ease of use, and an overall degree of validation. It also employs lower computational densities than other models such as large eddy current simulation (LES), and quarter models. The two-equation perturbation model shows a similar performance when inclined erosion is predicted, and computationally is less intense than a four-equation model or other complex perturbation models with mixed-phase flow simulation in terms of research, and industry.

The most commonly used method to calculate the particle effects is the Discere Phase Method (DPM) compared with the DEM method. However, since it does not take into account the effect of particles on the carrier or complex interactions between particles, if the particle concentration is expected to exceed 10%, particle monitoring structures such as the discrete element method (DEM) will be our best option.

Previous studies have shown that erosion studies are completed enough to grow single-phase flow. Therefore, further studies have more complex analyses with twin elbows and forms. On the other hand, in document-based double variance analysis, erosion analysis is limited to single-phase geometry with

Taheri Fard, A.

Pipe erosion under multiphase flow. A review;

2021; *AlfaBuild*; Volume 19 Article No 1901. doi: 10.57728/ALF.19.1



fixed bending. There is a rule of thumb in the industry that "if the distance between the bends exceeds 10 times the diameter of the pipe, the wear of the second bend can be compared with the first". Like grass, and other species.

## References

1. Parsi, M., Agrawal, M., Srinivasan, V., Vieira, R.E., Torres, C.F., McLaury, B.S., Shirazi, S.A. CFD simulation of sand particle erosion in gas-dominant multiphase flow. *Journal of Natural Gas Science, and Engineering*. 2015. 27. Pp. 706–718.
2. Finnie, I., Bailey, J.J. An experimental study of drill-string vibration. 1960.
3. Jordan, K.G. Erosion in multiphase production of oil & gas. *CORROSION* 98. 1998.
4. Levy, A. V. The platelet mechanism of erosion of ductile metals. *Wear*. 1986. 108(1). Pp. 1–21.
5. Bellman Jr, R., Levy, A. Erosion mechanism in ductile metals. *Wear*. 1981. 70(1). Pp. 1–27.
6. Finnie, I. The mechanism of erosion of ductile metals. 3rd US national congress of applied mechanics. 1958.
7. Hutchings, I.M., Winter, R.E. Particle erosion of ductile metals: a mechanism of material removal. *Wear*. 1974. 27(1). Pp. 121–128.
8. Hutchings, I.M. Deformation of metal surfaces by the oblique impact of square plates. *International Journal of Mechanical Sciences*. 1977. 19(1). Pp. 45–52.
9. Hutchings, I.M., Winter, R.E., Field, J.E. Solid particle erosion of metals: the removal of surface material by spherical projectiles. *Proceedings of the Royal Society of London. A. Mathematical, and Physical Sciences*. 1976. 348(1654). Pp. 379–392.
10. Andrews, D.R. An analysis of solid particle erosion mechanisms. *Journal of Physics D: Applied Physics*. 1981. 14(11). Pp. 1979.
11. Parsi, M., Vieira, R.E., Kesana, N., McLaury, B.S., Shirazi, S.A. Ultrasonic measurements of sand particle erosion in gas dominant multiphase churn flow in vertical pipes. *Wear*. 2015. 328. Pp. 401–413.
12. Levy, A. V. Erosion, and erosion-corrosion of metals. *Corrosion*. 1995. 51(11). Pp. 872–883.
13. Vieira, R.E., Mansouri, A., McLaury, B.S., Shirazi, S.A. Experimental, and computational study of erosion in elbows due to sand particles in air flow. *Powder technology*. 2016. 288. Pp. 339–353.
14. Sooraj, V.S., Radhakrishnan, V. Elastic impact of abrasives for controlled erosion in fine finishing of surfaces. *Journal of Manufacturing Science, and Engineering*. 2013. 135(5).
15. Mansouri, A., Arabnejad, H., Shirazi, S.A., McLaury, B.S. A combined CFD/experimental methodology for erosion prediction. *Wear*. 2015. 332. Pp. 1090–1097.
16. Meng, H.C., Ludema, K.C. Wear models, and predictive equations: their form, and content. *Wear*. 1995. 181. Pp. 443–457.
17. Shakesby, R.A., Coelho, C.O.A., Schnabel, S., Keizer, J.J., Clarke, M.A., Lavado Contador, J.F., Walsh, R.P.D., Ferreira, A.J.D., Doerr, S.H. A ranking methodology for assessing relative erosion risk, and its application to dehesas, and montados in Spain, and Portugal. *Land Degradation & Development*. 2002. 13(2). Pp. 129–140.
18. Mansouri, A., Shirazi, S.A., McLaury, B.S. Experimental, and numerical investigation of the effect of viscosity, and particle size on the erosion damage caused by solid particles. *Fluids Engineering Division Summer Meeting*. 2014. 46247. Pp. V01DT31A002.
19. API, R.P. 14E: Recommended practice for design, and installation of offshore production platform piping systems. API, Washington DC. 1991.
20. McLaury, B.S., Shirazi, S.A. An alternate method to API RP 14E for predicting solids erosion in multiphase flow. *J. Energy Resour. Technol.* 2000. 122(3). Pp. 115–122.
21. McLaury, B.S., Wang, J., Shirazi, S.A., Shadley, J.R., Rybicki, E.F. Solid particle erosion in long radius elbows, and straight pipes. *SPE annual technical conference, and exhibition*. 1997.
22. McLaury, B.S., Shirazi, S.A., Viswanathan, V., Mazumder, Q.H., Santos, G. Distribution of sand particles in horizontal, and vertical annular multiphase flow in pipes, and the effects on sand erosion. *Journal of energy resources technology*. 2011. 133(2).
23. Zhang, Y., Reuterfors, E.P., McLaury, B.S., Shirazi, S.A., Rybicki, E.F. Comparison of computed, and measured particle velocities, and erosion in water, and air flows. *Wear*. 2007. 263(1–6). Pp. 330–338.
24. Mohyaldin, M.E., Elkhatib, N., Ismail, M.C. Evaluation of different modeling methods used for erosion prediction. *Proceedings of the NACE Corrosion Changhai Conference & Expo*. 2011. Pp.

Taheri Fard, A.

Pipe erosion under multiphase flow. A review;

2021; *AlfaBuild*; Volume 19 Article No 1901. doi: 10.57728/ALF.19.1



- 1–19.
25. Shirazi, S.A., Shadley, J.R., McLaury, B.S., Rybicki, E.F. A procedure to predict solid particle erosion in elbows, and tees. 1995.
  26. Parsi, M., Kara, M., Agrawal, M., Kesana, N., Jatale, A., Sharma, P., Shirazi, S. CFD simulation of sand particle erosion under multiphase flow conditions. *Wear*. 2017. 376. Pp. 1176–1184.
  27. Salama, M.M., Venkatesh, E.S. Evaluation of API RP 14E erosional velocity limitations for offshore gas wells. *Offshore Technology Conference*. 1983.
  28. Rabinowicz, E. The wear equation for erosion of metals by abrasive particles. *International Conference on Erosion by Liquid, and Solid Impact, 5 th, Cambridge, England*. 1979. Pp. 31–38.
  29. Salama, M.M. An alternative to API 14E erosional velocity limits for sand-laden fluids. *J. Energy Resour. Technol.* 2000. 122(2). Pp. 71–77.
  30. Bourgoyne Jr, A.T. Experimental study of erosion in diverter systems due to sand production. *SPE/IADC drilling conference*. 1989.
  31. Svedeman, S.J. Criteria for sizing multiphase flowlines for erosive/corrosive service. *SPE Production & Facilities*. 1994. 9(01). Pp. 74–80.
  32. Weiner, P.D., Tolle, G.C. *Condensed Version of Detection, and Prevention of Sand Erosion of Production Equipment*. Texas A & M Research Foundation, 1976.
  33. Tatusov, R.L., Fedorova, N.D., Jackson, J.D., Jacobs, A.R., Kiryutin, B., Koonin, E. V, Krylov, D.M., Mazumder, R., Mekhedov, S.L., Nikolskaya, A.N. The COG database: an updated version includes eukaryotes. *BMC bioinformatics*. 2003. 4(1). Pp. 1–14.
  34. Zheng, D., Clark, M.K., Zhang, P., Zheng, W., Farley, K.A. Erosion, fault initiation, and topographic growth of the North Qilian Shan (northern Tibetan Plateau). *Geosphere*. 2010. 6(6). Pp. 937–941.
  35. Lynn, R.S., Wong, K.K., Clark, H.M. On the particle size effect in slurry erosion. *Wear*. 1991. 149(1–2). Pp. 55–71.
  36. Mazumder, Q.H., Shirazi, S.A., McLaury, B.S., Shadley, J.R., Rybicki, E.F. Development, and validation of a mechanistic model to predict solid particle erosion in multiphase flow. *Wear*. 2005. 259(1–6). Pp. 203–207.
  37. Arabnejad, H., Mansouri, A., Shirazi, S.A., McLaury, B.S. Development of mechanistic erosion equation for solid particles. *Wear*. 2015. 332. Pp. 1044–1050.
  38. Parsi, M., Jatale, A., Agrawal, M., Sharma, P. Effect of surface deformation on erosion prediction. *Wear*. 2019. 430. Pp. 57–66.
  39. Mazumder, Q.H. Effect of liquid, and gas velocities on magnitude, and location of maximum erosion in U-bend. 2012.
  40. Ishii, M., Mishima, K. Droplet entrainment correlation in annular two-phase flow. *International Journal of Heat, and Mass Transfer*. 1989. 32(10). Pp. 1835–1846.
  41. Mazumder, Q.H., Shirazi, S.A., McLaury, B.S. A mechanistic model to predict erosion in multiphase flow in elbows downstream of vertical pipes. *CORROSION* 2004. 2004.
  42. Mazumder, Q.H., Santos, G., Shirazi, S.A., McLaury, B.S. Effect of sand distribution on erosion in annular three-phase flow. *Fluids Engineering Division Summer Meeting*. 2003. 36967. Pp. 871–880.
  43. Mazumder, Q.H., Ahmed, K., Zhao, S. Experimental investigation of solid particle erosion in S-bend. *Journal of Fluids Engineering*. 2016. 138(4).
  44. Mazumder, Q.H., Shirazi, S.A., McLaury, B. Experimental investigation of the location of maximum erosive wear damage in elbows. *Journal of Pressure Vessel Technology*. 2008. 130(1).
  45. Chen, T., Niu, R., Li, P., Zhang, L., Du, B. Regional soil erosion risk mapping using RUSLE, GIS, and remote sensing: a case study in Miyun Watershed, North China. *Environmental Earth Sciences*. 2011. 63(3). Pp. 533–541.
  46. Zhang, J., McLaury, B.S., Shirazi, S.A. Application, and experimental validation of a CFD based erosion prediction procedure for jet impingement geometry. *Wear*. 2018. 394. Pp. 11–19.
  47. Zhou, M., Liu, H., Kang, C., Wei, X. Resistance of curved surfaces to the cavitation erosion produced through high-pressure submerged waterjet. *Wear*. 2019. 440. Pp. 203091.
  48. Kang, R., Liu, H. An integrated model of predicting sand erosion in elbows for multiphase flows. *Powder Technology*. 2020. 366. Pp. 508–519.
  49. Kang, R., Liu, H. A probability model of predicting the sand erosion in elbows for annular flow. *Wear*. 2019. 422. Pp. 167–179.
  50. Singh, R., Mazumdar, D. Mathematical modeling, and validation of wall shear stress in gas stirred vessels. *ISIJ international*. 2008. 48(7). Pp. 1033–1035.

Taheri Fard, A.

Pipe erosion under multiphase flow. A review;

2021; *AlfaBuild*; Volume 19 Article No 1901. doi: 10.57728/ALF.19.1



51. Graham, L.J.W., Lester, D., Wu, J. Slurry erosion in complex flows: experiment, and CFD. Proceedings of the 7th International Conference on CFD in the Minerals, and Process Industries. 2009. Pp. 1–6.
52. Graham, L., Wong, C.Y., Lester, D., Wu, J. Laboratory Modeling of Equipment Erosion by Sand Particles. SPE Annual Technical Conference, and Exhibition. 2009.
53. Kesana, N.R. Erosion in multiphase pseudo slug flow with emphasis on sand sampling, and pseudo slug characteristics. The University of Tulsa, 2013. ISBN:1303376660.
54. Kesana, N.R., Throneberry, J.M., McLaury, B.S., Shirazi, S.A., Rybicki, E.F. Effect of particle size, and liquid viscosity on erosion in annular, and slug flow. Journal of Energy Resources Technology. 2014. 136(1).
55. Vieira, R.E., Kesana, N.R., McLaury, B.S., Shirazi, S.A. Sand erosion in multiphase flow for low-liquid loading, and annular conditions. ASME International Mechanical Engineering Congress, and Exposition. 2012. 45233. Pp. 2445–2454.
56. Vieira, R.E., Parsi, M., Zahedi, P., McLaury, B.S., Shirazi, S.A. Ultrasonic measurements of sand particle erosion under upward multiphase annular flow conditions in a vertical-horizontal bend. International Journal of Multiphase Flow. 2017. 93. Pp. 48–62.
57. Zhang, Y., McLaury, B.S., Shirazi, S.A. Improvements of particle near-wall velocity, and erosion predictions using a commercial CFD code. Journal of Fluids Engineering. 2009. 131(3).
58. Wu, Y., Hong, S., Zhang, J., He, Z., Guo, W., Wang, Q., Li, G. Microstructure, and cavitation erosion behavior of WC–Co–Cr coating on 1Cr18Ni9Ti stainless steel by HVOF thermal spraying. International Journal of Refractory Metals, and Hard Materials. 2012. 32. Pp. 21–26.
59. Jafari, M., Mansoori, Z., Avval, M.S., Ahmadi, G. The effects of wall roughness on erosion rate in gas–solid turbulent annular pipe flow. Powder Technology. 2015. 271. Pp. 248–254.
60. Chen, J., Wang, Y., Li, X., He, R., Han, S., Chen, Y. Reprint of “Erosion prediction of liquid-particle two-phase flow in pipeline elbows via CFD–DEM coupling method.” Powder Technology. 2015. 282. Pp. 25–31.
61. Zahedi, P., Karimi, S., Mahdavi, M., McLaury, B.S., Shirazi, S.A. Parametric analysis of erosion in 90 degree, and long radius bends. Fluids Engineering Division Summer Meeting. 2016. 50282. Pp. V01AT06A003.
62. Vieira, R.E. Sand erosion model improvement for elbows in gas production, multiphase annular, and low-liquid flow. The University of Tulsa, 2014. ISBN:1321307616.
63. Grant, G., Tabakoff, W. Erosion prediction in turbomachinery resulting from environmental solid particles. Journal of Aircraft. 1975. 12(5). Pp. 471–478.
64. Mahdavi, M., Karimi, S., Shirazi, S.A., McLaury, B.S. Parametric study of erosion under high concentrated slurry: experimental, and numerical analyses. ASME 2016 Fluids Engineering Division Summer Meeting collocated with the ASME 2016 Heat Transfer Summer Conference, and the ASME 2016 14th International Conference on Nanochannels, Microchannels, and Minichannels. 2016.
65. Ashrafizadeh, H., Ashrafizadeh, F. A numerical 3D simulation for prediction of wear caused by solid particle impact. Wear. 2012. 276. Pp. 75–84.
66. Xu, L., Zhang, Q., Zheng, J., Zhao, Y. Numerical prediction of erosion in elbow based on CFD-DEM simulation. Powder Technology. 2016. 302. Pp. 236–246.
67. Peng, W., Cao, X., Hou, J., Ma, L., Wang, P., Miao, Y. Numerical prediction of solid particle erosion under upward multiphase annular flow in vertical pipe bends. International Journal of Pressure Vessels, and Piping. 2021. Pp. 104427.
68. Peng, W., Cao, X. Numerical simulation of solid particle erosion in pipe bends for liquid–solid flow. Powder technology. 2016. 294. Pp. 266–279.
69. Al-Khayat, R.H., Al-Baghdadi, M.A.R.S., Neama, R.A., Al-Waily, M. Optimization CFD Study of Erosion in 3D Elbow During Transportation of Crude Oil Contaminated with Sand Particles. International Journal of Engineering & Technology. 2018. 7(03). Pp. 1420–1428.
70. Al-Waily, M., Al-Baghdadi, M.A.R.S., Al-Khayat, R.H. Flow Velocity, and Crack Angle Effect on Vibration, and Flow Characterization for Pipe Induce Vibration. International Journal of Mechanical & Mechatronics Engineering IJMME-IJENS. 2017. 17(05). Pp. 19–27.
71. Peng Jr, D., Pak, A., Chinello, L., Wood, T., Low, A. Advances in multiphase flow CFD erosion analysis. Offshore Technology Conference. 2013.
72. Oka, Y.I., Okamura, K., Yoshida, T. Practical estimation of erosion damage caused by solid particle impact: Part 1: Effects of impact parameters on a predictive equation. Wear. 2005. 259(1–

Taheri Fard, A.

Pipe erosion under multiphase flow. A review;

2021; *AlfaBuild*; Volume 19 Article No 1901. doi: 10.57728/ALF.19.1





- 6). Pp. 95–101.
73. Oka, Y.I., Yoshida, T. Practical estimation of erosion damage caused by solid particle impact: Part 2: Mechanical properties of materials directly associated with erosion damage. *Wear*. 2005. 259(1–6). Pp. 102–109.
74. Nguyen, Q.B., Nguyen, V.B., Lim, C.Y.H., Trinh, Q.T., Sankaranarayanan, S., Zhang, Y.W., Gupta, M. Effect of impact angle, and testing time on erosion of stainless steel at higher velocities. *Wear*. 2014. 321. Pp. 87–93.
75. Nguyen, V.B., Nguyen, Q.B., Liu, Z.G., Wan, S., Lim, C.Y.H., Zhang, Y.W. A combined numerical–experimental study on the effect of surface evolution on the water–sand multiphase flow characteristics, and the material erosion behavior. *Wear*. 2014. 319(1–2). Pp. 96–109.
76. Deng, T., Chaudhry, A.R., Patel, M., Hutchings, I., Bradley, M.S.A. Effect of particle concentration on erosion rate of mild steel bends in a pneumatic conveyor. *Wear*. 2005. 258(1–4). Pp. 480–487.
77. Sedrez, T.A., Shirazi, S.A., Rajkumar, Y.R., Sambath, K., Subramani, H.J. Experiments, and CFD simulations of erosion of a 90 elbow in liquid-dominated liquid-solid, and dispersed-bubble-solid flows. *Wear*. 2019. 426. Pp. 570–580.
78. Sedrez, T.A., Rajkumar, Y.R., Shirazi, S.A., Sambath, K., Subramani, H.J. CFD simulations, and experiments of sand erosion for liquid dominated multiphase flows in an elbow. 11th North American Conference on Multiphase Production Technology. 2018.
79. Asgharpour, A., Zahedi, P., Arabnejad Khanouki, H., Shirazi, S.A., McLaury, B.S. Experimental, and numerical study on solid particle erosion in elbows mounted in series. ASME 2017 Fluids Engineering Division Summer Meeting. 2017.
80. Farokhipour, A., Mansoori, Z., Saffar-Avval, M., Rasoulia, M.A., Rasteh, A., Shirazi, S.A., Ahmadi, G. A Numerical Study of Sand Particle Erosion in Elbow, and a Series of Plugged Tees in Gas-Particle Two-Phase Flow. ASME 2018 5th Joint US-European Fluids Engineering Division Summer Meeting. 2018.